Published in final edited form as:
Biomaterials. 2012 October ; 33(28): 6682–6690. doi:10.1016/j.biomaterials.2012.06.005.

Cartilage-like mechanical properties of poly (ethylene glycol)-diacrylate hydrogels

Quynhhoa T. Nguyen[a], **Yongsung Hwang**[c], **Albert C. Chen**[a], **Shyni Varghese**[a,c,d], and **Robert L. Sah**[a,b,c,d,*]

[a]Department of Bioengineering, University of California – San Diego, La Jolla, CA, USA

[b]Department of Orthopaedic Surgery, University of California – San Diego, La Jolla, CA, USA

[c]Department of Materials Science and Engineering Program, University of California – San Diego, La Jolla, CA, USA

[d]Center for Musculoskeletal Research – Institute of Engineering in Medicine, University of California – San Diego, La Jolla, CA, USA

Abstract

Hydrogels prepared from poly-(ethylene glycol) (PEG) have been used in a variety of studies of cartilage tissue engineering. Such hydrogels may also be useful as a tunable mechanical material for cartilage repair. Previous studies have characterized the chemical and mechanical properties of PEG-based hydrogels, as modulated by precursor molecular weight and concentration. Cartilage mechanical properties vary substantially, with maturation, with depth from the articular surface, in health and disease, and in compression and tension. We hypothesized that PEG hydrogels could mimic a broad range of the compressive and tensile mechanical properties of articular cartilage. The objective of this study was to characterize the mechanical properties of PEG hydrogels over a broad range and with reference to articular cartilage. In particular, we assessed the effects of PEG precursor molecular weight (508 Da, 3.4 kDa, 6 kDa, and 10 kDa) and concentration (10–40%) on swelling property, equilibrium confined compressive modulus (H_{A0}), compressive dynamic stiffness, and hydraulic permeability (k_{p0}) of PEG hydrogels in static/dynamic confined compression tests, and equilibrium tensile modulus (E_{ten}) in tension tests. As molecular weight of PEG decreased and concentration increased, hydrogels exhibited a decrease in swelling ratio (31.5–2.2), an increase in H_{A0} (0.01–2.46 MPa) and E_{ten} (0.02–3.5 MPa), an increase in dynamic compressive stiffness (0.055–42.9 MPa), and a decrease in k_{p0} (1.2×10^{-15} to 8.5×10^{-15} $m^2/(Pa\ s)$). The frequency-dependence of dynamic compressive stiffness amplitude and phase, as well as the strain-dependence of permeability, were typical of the time- and strain-dependent mechanical behavior of articular cartilage. H_{A0} and E_{ten} were positively correlated with the final PEG concentration, accounting for swelling. These results indicate that PEG hydrogels can be prepared to mimic many of the static and dynamic mechanical properties of articular cartilage.

Keywords

PEG; Biomechanics; Crosslink; Compression; Tension; Modulus

*Corresponding author. Department of Bioengineering, Mail Code 0412, University of California – San Diego, 9500 Gilman Drive, La Jolla, CA 92093-0412, USA. Tel.: +1 858 534 0821; fax: +1 858 822 1614. rsah@ucsd.edu (R.L. Sah).

1. Introduction

The ability of hydrogels to provide mechanical support and mechanical cues is particularly important for tissue engineering with cell types that are normally subjected to load. Poly (ethylene glycol) (PEG) hydrogels have been used extensively for *in vivo* and *in vitro* tissue engineering of cartilage, which normally bears both compressive and tensile load. PEG hydrogels provide a three-dimensional environment, sufficiently resembling that of native cartilaginous tissues to maintain differentiated cells in a chondrogenic phenotype [1-3] and to examine chondrogenic differentiation, for example, by mesenchymal stem cells [3-6]. PEG hydrogels are able to maintain cells viable and synthesizing cartilaginous matrix [1-8].

PEG hydrogels are fluid-filled crosslinked three-dimensional networks, consisting of covalently bonded PEG chains, and can be formed from multifunctional PEG precursors. PEG hydrogels can be fabricated by photopolymerization of PEG precursors modified with either acrylate or methacrylate moieties in the presence of photoinitiators [9]. Upon exposure to UV light, photoinitiators are fragmented to yield free radicals. These radicals attack carbon–carbon double bonds present in the acrylate groups, initiating polymerization to form a hydrogel network. When exposed to aqueous solvents, the crosslinked network swells until the retractive (elastic) forces of the polymer chain are balanced by swelling forces of the network [10]. A more tightly crosslinked hydrogel will have larger retractive forces, resulting in less water being imbibed within the network [11].

The mechanical properties of articular cartilage have been characterized extensively and vary substantially during growth and in adults, as well as in health and disease [12-22]. The stiffness of articular cartilage varies markedly with frequency and test conditions. Such mechanical behavior can be described well by intrinsic elastic material properties and strain-dependent hydraulic permeability [13,15-20,22], with consideration of structural dimensions and physical boundary conditions. The compressive modulus and permeability of cartilage vary with depth from the articular surface. The equilibrium confined compression modulus (H_{A0}) of cartilage ranges from 0.08 to 2.1 MPa from superficial to deep layers of adult bovine cartilage [17] and increases with maturation [15]. The dynamic compressive stiffness of articular cartilage increases substantially with frequency and strain rate in the confined configuration [13,15,16]. The equilibrium tensile modulus (E_{ten}) of mature adult cartilage is higher than the compressive modulus, varying in human articular cartilage from 25 MPa in the superficial layer to 4.8 MPa in the deep layer [21] and increasing with maturation [12]. The hydraulic permeability (k_p), a measure of the ease with which fluid flows through the tissue when driven by a pressure gradient [13,22], is strain-dependent and can be inferred from dynamic compression tests. The k_p of cartilage varies with depth from the articular surface [13,22] as well as with compressive strain [18], ranging from 0.3×10^{-17} to 4.6×10^{-15} $m^2/(Pa\ s)$ in adult bovine articular cartilage [13,15].

The structure and swelling properties of PEG hydrogels are affected by molecular weight and concentration of the precursors [23-27]. Mesh size (ξ), the average distance between adjacent crosslinks, is a measure of the space available between PEG chains. Mesh size increases with molecular weight, for example, doubling from 7.6 nm to 16 nm when the molecular weight of PEG increases from 860 Da to 10 kDa [23]. In contrast, ξ decreases as PEG concentration increases, for example, halving from 14–16 to 6–8 nm as the concentration of 3 kDa PEG increases from 10 to 20% w/v [24,26]. PEG molecular weight and concentration have similar effects on the average molecular weight between crosslinks (M_c), a measure of the degree of crosslinking of PEG hydrogels [23,24]. Concomitantly, the volumetric swelling ratio, the volume of hydrogel relative to the volume of polymer, increases with PEG molecular weight [23,25] and decreases with PEG concentration [24,26,27].

A variety of mechanical properties of PEG hydrogels are also modulated by molecular weight and concentration of PEG precursors, over the ranges studied previously (Table 1, Fig. 1) [1,8,23-32]. PEG hydrogels with higher concentration have higher compressive modulus as assessed by a constant rate compression test [1,24,28,31,32] and higher tensile modulus as assessed by constant rate extension test [23,25]. At similar PEG concentration, hydrogels with low molecular weight are more brittle, as indicated by tensile failure at lower strain [8,23-25,27-29,31,32]. For example, hydrogels fabricated from PEG with low molecular weight (1 kDa) had higher tensile ramp modulus (90 kPa) and lower fracture strain (30%) than hydrogels formed with 4 or 10 kDa PEG [23]. In those studies, mechanical properties of PEG hydrogels have been assessed by a compression test with a constant rate (strain or stress) until failure. The ramp modulus was determined as the slope of the linear region of the resulted stress–strain curve [23-25,27-30,33]; however, this property is generally greater than the intrinsic (equilibrium) material elastic modulus. Although the results from such studies have provided useful information on rate-dependent structural mechanical properties, a more comprehensive mechanical characterization of the intrinsic material properties and viscoelastic mechanical properties of PEG hydrogels would be useful; such information would guide the selection and design of appropriate scaffolds for tissue engineering applications, both for macroscopic load-bearing properties and for mechanical cues transmitted to cells by matrix stiffness [34] in the absence or presence of external loads. In addition, since certain types of external loads are periodic, assessment of dynamic properties over a range of frequencies is also of interest.

We hypothesized that the cartilaginous properties of PEG hydrogels could be modulated by varying the molecular weight and the concentration of PEG precursors to achieve compressive properties characteristic of articular cartilage during growth and in adults, as well as in health, disease, and repair. The aims of the present study were to determine the effects of PEG molecular weight (508 Da, 3.4 kDa, 6 kDa, and 10 kDa) and PEG concentration (10–40%) on compressive dynamic stiffness, equilibrium confined compressive modulus (H_{A0}), and hydraulic permeability (k_p) of PEG hydrogels in static and dynamic confined compression tests, and equilibrium tensile modulus (E_{ten}) in equilibrium tensile tests.

2. Methods

2.1. PEG hydrogel preparation

PEG diacrylate of low molecular weight (number-average molecular weight, M_n, of 508 Da, PEG_{508}) was purchased from Sigma–Aldrich (St Louis, MO). Higher molecular weight (M_n = 3400 Da ($PEG_{3.4k}$), 6000 Da (PEG_{6k}), and 10,000 Da (PEG_{10k})) PEG diacrylate was synthesized as described previously [35] and purified by precipitation in diethyl ether followed by gel filtration chromatography (Sephadex® G-25) and then dialysis with molecular weight cut-off of 500 Da against deionized H_2O (Spectrum, Rancho Dominguez, CA). IRGACURE 2959 (I2959, Ciba Specialty Chemicals, Basel, Switzerland) was used as a photoinitiator.

PEG hydrogels were fabricated from 10, 20, 30, or 40% v/v of PEG_{508} or 10, 20, 30, or 40% w/w of $PEG_{3.4k}$, PEG_{6k}, and PEG_{10k} in phosphate buffered saline (PBS), with 0.1 %w/w I2959. PEG solutions were injected into a rectangular mold consisting of two parallel glass slides separated by 1 mm and photopolymerized using UV irradiation (365 nm) at 45 mW/cm^2 (Blak-Ray Model XX-15L UV lamp) for 5 min. Then, the PEG hydrogels (~1 ml, each) were removed from the mold and rinsed 3 times with PBS (~30 ml per rinse) at room temperature over 48 h to remove un-reacted precursors and to reach an equilibrium swelling state.

2.2. Compositional and structural analyses

Samples were analyzed for swelling ratio, swollen PEG concentration ($[PEG]_{swollen}$), average molecular weight between crosslinks (M_c, g/mol), and mesh size (ξ, nm). Samples were measured for thickness, weighed wet, lyophilized overnight, and weighed dry. The swelling ratio and water content were computed from wet weight (ww) and dry weight (dw) measurements. $[PEG]_{swollen}$ was calculated as the ratio of dry weight to hydrogel volume, calculated from the thickness and diameter. The average molecular weight between crosslinks (M_c) and mesh size (ξ) were calculated from the polymer volume fractions in the relaxed and swollen state ($\upsilon_{2,r}$ and $\upsilon_{2,s}$, respectively), specific volume of PEG-DA in its amorphous state ($\nu = 0.893$ cm^3/g), the Flory–Huggin's polym–resolvent interaction parameter ($\chi = 0.426$), and molar volume of the solvent (18 cm^3/mol), using the Peppas–Merrill model as described previously [36-38].

2.3. Mechanical testing

Samples were characterized mechanically using equilibrium and dynamic compression and tensile test protocols [13,15].

2.3.1. Confined compression testing—Confined compression (CC) tests were performed to assess aggregate modulus, dynamic stiffness at 0.0003–3 Hz or 0.01–1 Hz, and hydraulic permeability at 15 and 30% axial strain and extrapolated to the free swelling condition. Hydrogel disks of 6.4 mm in diameter were punched out from each hydrogel formulation ($n = 4$ per experimental group) and measured for thickness and wet weight. Each disk was then placed within a confining ring between two porous platens (pore size 2 μm) submerged in PBS and affixed to a materials testing machine (Dynastat, Northern Industrial, Albany, NY). The test sequence consisted of two consecutive constant rate ramps (at 0.0125%/s over 1200 s) to 15 and 30% axial strains, with stress relaxation for at least 1200 s to equilibrium (until a relaxation criteria of less than 0.003 MPa change in stress in 180 s was met). At each static offset, oscillatory displacements with an amplitude of 0.5% and frequencies of 0.01, 0.1, and 1 Hz were applied. The compressive aggregate modulus at the free swelling thickness (H_{A0}), dynamic stiffness (amplitude and phase) at each frequency and compression offset, hydraulic permeability at free swelling thickness and at each compression offset (k_{p0} and k_p, respectively) were estimated from fits of the static and dynamic data, as described previously [13]. Hydrogels with high concentration (40% w/v) of $PEG_{3.4k}$ and PEG_{508} ($n = 3$ per group) were tested dynamically over an extended frequency range (0.0003, 0.001, 0.01, 0.1,1, and 3 Hz) to further elucidate the characteristic frequency-dependence of compressive stiffness.

2.3.2. Equilibrium tensile testing—Tensile tests were performed to assess tensile modulus. Tapered specimens ($n = 4$) with a gage region of approximately 4 mm × 1 mm × 1 mm (length × width × height) were prepared from 30% w/w hydrogels at each of the molecular weights, and also from $PEG_{3.4k}$ at 10, 20, 30, and 40% w/w concentrations. Thickness and width of the gage region were measured prior to tensile tests. Samples were subjected to a tare load of 2 g (equivalent to a stress of 0.02 MPa), elongated at constant rate of 10 μm/s to strains that allowed reproducible load measurements without fracture, 5% for PEG_{508},10 and 20% for $PEG_{3.4k}$ and PEG_{6k}, and 20 and 40% for PEG_{10k} with stress relaxation for at least 900 s to equilibrium (until a relaxation criteria of less than 0.010 MPa change in stress in 60 s was met). Throughout mechanical testing, samples were kept hydrated with PBS at room temperature. It was observed that on average, the load relaxed by ~15% at equilibrium. Equilibrium tensile modulus (E_{ten}) was calculated as the slope of the equilibrium stress–strain data at 0–5% (PEG_{508}), 0–10–20% ($PEG_{3.4k}$ and PEG_{6k}), or 0–20–40% (PEG_{10k}) by linear regression. Since analysis indicated that the peak tensile loads (at the end of each ramp) were within 15% of the equilibrium loads (data not shown), the

equilibrium loads also provided an index of dynamic tensile stiffness, and the latter is not presented separately.

2.4. Statistical analysis

Data are presented as mean ± SEM. The effects of PEG molecular weight and concentration on the bulk mechanical properties (i.e. H_{A0}, k_{p0}, and E_{ten}), and on structural properties (i.e. thickness, swelling ratio, $[PEG]_{swollen}$, M_c, and ξ) of PEG hydrogels were assessed by two-way ANOVA. The strain- and frequency-dependence effects on k_p and dynamic stiffness amplitude and phase were assessed by two-way repeated measures ANOVA with the compressive strain offset and frequency as repeated factors. For certain data (mesh size, dynamic stiffness, and k_p) that exhibited variation that was substantial and approximately proportional to the mean, logarithmic transformation was performed to improve normality before statistical analyses [39]. Significance levels were set at $p < 0.05$.

3. Results

3.1. Compositional and structural properties

The thickness, swelling ratio, and swollen concentration ($[PEG]_{swollen}$) of hydrogels varied with PEG molecular weight and concentration. Thickness increased with increasing PEG molecular weight and concentration (each, $p < 0.001$, Fig. 2A), and inverse to this $[PEG]_{swollen}$ decreased with PEG molecular weight but increased with PEG concentration ($p < 0.001$, Fig. 2B). In contrast, while swelling ratio increased with PEG molecular weight, it decreased with PEG concentration ($p < 0.001$, Fig. 2C). The difference in thickness between hydrogels of PEG_{10k} and lower molecular weight (PEG_{508}, $PEG_{3.4k}$ or PEG_{6k}) was more pronounced than the thickness difference between PEG_{508}, $PEG_{3.4k}$ and PEG_{6k} hydrogels (Fig. 2A). Only PEG_{508} hydrogels had $[PEG]_{swollen}$ (Fig. 2B) and thickness (Fig. 2A) similar to their initial concentration and dimension, respectively. In contrast, PEG hydrogels of higher molecular weight had $[PEG]_{swollen}$ that was lower than initial values. Thus, the equilibrated state of PEG hydrogels reflected variable degrees of swelling.

The computed molecular weight, M_c, and mesh size, ξ, were increased with increasing PEG molecular weight and decreased with increasing PEG concentration. M_c was lower by 20–70% when PEG concentration increased from 10 to 40% and was higher by 20-to 40-fold when PEG molecular weight increased from 508 to 10,000 (each, $p < 0.001$, Table 2). With a similar trend, ξ increased from 1.7 nm to 12.4 nm as molecular weight increased from 508 to 10,000 Da for 10% w/w hydrogels ($p < 0.001$) and ξ was lower as PEG concentration increased from 10% to 30% or 40% ($p < 0.001$). Thus, the microstructure of the hydrogels also varied substantially depending on PEG molecular weight and concentration. Similar trend was observed for water content of these hydrogels (both, $p < 0.001$).

3.2. Confined compression properties

The compressive modulus of hydrogels, determined from equilibrium stress–strain data, also varied with PEG concentration and molecular weight. The modulus, H_{A0}, was higher with increasing PEG concentration or decreasing PEG M_n ($p < 0.001$, Fig. 3). The effect of M_n on H_{A0} was especially pronounced with PEG of lower molecular weight (PEG_{508}) and at high concentration (30%).

The amplitude and phase of dynamic stiffness were dependent on test frequency (both, $p < 0.001$), PEG concentration (both, $p < 0.001$), and PEG molecular weight (both, $p < 0.001$) (Fig. 4). There were interactive effects on stiffness amplitude of frequency, molecular weight, and concentration at 15% offset ($p < 0.05$), and interactive effects of frequency and molecular weight at 30% offset ($p < 0.001$). At any given frequency (0.01, 0.1, or 1 Hz) at

15% static offset, dynamic stiffness amplitude decreased with PEG M_n and increased with PEG concentration (Fig. 4A–C), and similar effects were apparent at 30% static offset (Fig. 4D–F). In general, stiffness at 15% static offset was lower than that at 30% offset ($p < 0.001$). Dynamic stiffness phase was also affected by frequency, PEG molecular weight, and PEG concentration (Fig. 4G–L). Dynamic phase generally decreased from peak values of 15–40° with test frequency and PEG molecular weight. Thus, PEG hydrogels exhibited frequency-dependent dynamic stiffness, indicative of viscoelastic behavior.

The frequency-dependent mechanical behavior of 40% PEG hydrogels of PEG_{508} and $PEG_{3.4k}$ was clarified in confined compression tests with an extended frequency range to a low of 0.0003 Hz and a high of 3 Hz (Fig. 5). At 15% strain offset, the amplitude of dynamic stiffness increased steadily with frequency and reached a peak at frequencies of 0.001 Hz for PEG_{508} and 0.1 Hz for $PEG_{3.4k}$ (Fig. 5A, B). At 30% static strain, the stiffness increased steadily with frequency. The phase of dynamic stiffness generally decreased with increasing frequency. The phase shift reached a peak of ~30° at 0.0003–0.001 Hz and 30% offset for both PEG_{508} and $PEG_{3.4k}$ and then decreased with increasing frequency (Fig. 5C, D).

The hydraulic permeability, determined from the static and dynamic data, was dependent on PEG formulation and also on the offset strain. At free swelling thickness, k_{p0} decreased with increasing PEG concentration ($p < 0.05$), but did not vary with M_n ($p = 0.68$, Fig. 6). In addition, k_p was strain-dependent ($p < 0.001$), with k_p being ~25– ~900% higher at 15% offset than at 30% offset.

Correlation analysis revealed dependences of compressive properties on actual PEG content. The H_{A0} versus $[PEG]_{swollen}$ showed a strong positive correlation that was fit well by a second order polynomial function ($R^2 = 0.96$) (Fig. 7). H_{A0} also increased with dry weight ($R^2 = 0.95$, data not shown).

3.3. Equilibrium tensile properties

The equilibrium tensile modulus, E_{ten}, of PEG hydrogels varied both with molecular weight and concentration. As molecular weight increased from 508 to 10,000, at 30% w/w, E_{ten} decreased more than 10-fold from 3.50 MPa to 0.03 MPa ($p < 0.001$, Fig. 8A). As concentration increased from 10 to 40% of $PEG_{3.4k}$, E_{ten} increased from 0.04 to 0.89 MPa ($p < 0.001$, Fig. 8B). E_{ten} was positively correlated with $[PEG]_{swollen}$ [%w/v], calculated as the percentage of dry weight to estimated volume ($R^2 = 0.999$, Fig. 8C).

4. Discussion

This study elucidated the equilibrium and dynamic mechanical properties in compression and the equilibrium properties in tension of hydrogels formed from PEG diacrylate over a range of molecular weights (PEG_{508}, $PEG_{3.4k}$, PEG_{6k}, and PEG_{10k}) and concentrations (10–40%). As PEG molecular weight increased, PEG hydrogels increased in free-swelling thickness, swelling ratio, M_c and ξ (Fig. 2, Table 2), and diminished in load-bearing properties (decrease in H_{A0}, increase in k_p, and decrease in E_{ten}) (Figs. 3, 6 and 8). As the concentration of PEG precursors was increased, PEG hydrogels increased in thickness, decreased in swelling ratio, M_c, and ξ (Fig. 2, Table 2), and increased in load-bearing properties (increase in H_{A0}, decrease in k_p, and increase in E_{ten}) (Figs. 3, 6, and 8). PEG hydrogels tested in this study exhibited frequency-dependent dynamic stiffness, and strain- and frequency-dependent permeability (Figs. 4-6), typical of cartilage poroelastic behavior. Thus, the compressive and tensile mechanical properties of PEG hydrogels spanned much of the range of native articular cartilage (Fig. 1).

The current study focused on selected mechanical properties of PEG hydrogels. The mechanical properties determined here provide a substantial characterization of the elastic properties of PEG hydrogels. In addition to compressive and tensile elastic properties, shear modulus or Poisson's ratio would be useful to assess to more fully define the mechanical properties of PEG hydrogels. In PEG-based degradable hydrogels with proteolytic degradation sites, the degree of degradation could also affect the material properties of hydrogels [40]. The concentration of PEG diacrylate at equilibrium swollen state ($[PEG]_{swollen}$) was markedly lower than the initial concentration due to swelling. Therefore, to determine a concentration and molecular weight of PEG to fabricate a hydrogel with specific modulus or permeability, the extent of swelling should be considered.

The values of H_{A0} determined in the present study are consistent with, and extend, the compressive data in the literature for PEG hydrogels (Table 1, Fig. 1). The differences between compressive modulus measured here and those assessed previously are likely due to differences in test and data reduction methods for equilibrium and dynamic compression protocols, with the latter being at a variety of strain rates. Distinguishing between equilibrium and dynamic properties is important from both theoretical and practical standpoints. Theoretically, the confined compression behavior of poro-elastic materials is determined by equilibrium modulus and hydraulic permeability, as well as strain-dependent behavior and the imposed boundary conditions [13,16-20]. Practically, dynamic stiffness relates to the function of cartilage in a physiological situation. The range of PEG equilibrium modulus in compression (0.01–2.46 MPa, Figs. 1 and 3) covers much of the range of the mechanical properties of cartilaginous biological tissues, such as articular cartilage in the immature (0.1–0.3 MPa) [15] and mature state (0.19–2.1 MPa) [13,15-17,20] and also meniscus (0.38−0.49 MPa) [41] and intervertebral disc (IVD) (0.38–1.01 MPa) [14,42,43].

The hydraulic permeability of PEG hydrogels, ranging from 10^{-13} to 10^{-16} (m^2/Pa s), also spans the range of values of native articular cartilage. Low k_p values of PEG hydrogels correspond to permeability of cartilage from deep layer (0.5–0.76 × 10^{-15} m^2/Pa s at 0% strain) or when under higher compression (0.47–1.5 × 10^{-15} m^2/Pa s at 20–30% strain) [13,18]. The higher k_p of PEG-based hydrogels are somewhat similar to that of cartilage layers at or near the articular surface (4.6–7.6 × 10^{-15} m^2/Pa s) [13,16]. The values are also in range with those of meniscus (0.63–1.03 × 10^{-15} m^2/Pa s) [41] and IVD (0.2–0.9 × 10^{-15} m^2/Pa s) [14,43]. The marked decrease in hydraulic permeability with increasing compression and PEG concentration is also consistent with the strain-dependent permeability of articular cartilage [13,18,19] and the molecular basis of hydraulic permeability [44,45].

The values of tensile moduli of PEG hydrogels determined here also extend the range of values reported in literature (Table 1, Fig. 1) and cover some of the range of native articular cartilage. E_{ten} of 20% $PEG_{3.4k}$ hydrogels, 0.33 MPa, was consistent with a report of quasi-static tensile modulus [27]. The increase in equilibrium tensile modulus with concentration and decrease with molecular weight is consistent with trends from previous studies [23,27]. The equilibrium tensile modulus (0.02–3.5 MPa) of PEG hydrogels examined in this study had some overlap with tensile properties of articular cartilage of fetal bovine knee joints (0.5–1 MPa), but was lower than that of calf or adult bovine articular cartilage (1.8–5.4 MPa) [12] and substantially lower than that of adult human articular cartilage [21]. Recapitulating the fiber-reinforced nature of cartilage with the addition of fibers into the hydrogel network could enhance its tensile stiffness and strength [46].

A variety of biomechanical features of PEG hydrogels are consistent with the behavior of a biphasic, poro-elastic material. In dynamic compression, PEG hydrogels exhibited a frequency-dependent response (Figs. 4–6), consistent with the frequency-dependent [13,20]

and time-dependent [16] responses of articular cartilage. The mechanical properties of PEG-based hydrogels are dependent on precursor concentration and molecular weight, analogous to that of other hydrogels, such as agarose, alginate, and polypeptides [47-49]. The positive correlation of H_{A0} and k_p with the concentration of PEG at the swollen state suggested that the amount of material present in a specified volume, rather than the molecular weight or concentration of the macromer component *per se*, was a primary determinant of hydrogel confined compression mechanical properties.

The increase in swelling ratio with increasing molecular weight or decreasing concentration was consistent with, and extend, results of previous studies [23,24,27]. In general, M_c and ξ (Table 2) were consistent with and extended the range of values reported in the literature [24,26,36]. Hydrogels made with PEG–diacrylate precursors with molecular weight of 10,000 have ξ values of 85–123 Å, similar to those (40–120 Å) of PEG-dimethacrylate hydrogels with molecular weight of 3400 [26], suggesting that the functional groups (i.e. acrylate, methacrylate, or other types) at the ends of PEG molecules may affect the hydrogel's three-dimensional crosslinked structure. The effects of concentration and molecular weight of PEG precursor on M_c and ξ observed in this study were similar to those described previously for PEG-based hydrogels with different functional moieties [24,26,36]. In addition, PEG molecular weight and PEG concentration had similar effects on ξ and on k_p (Table 2 and Fig. 6), consistent with the hydraulic permeability of hydrogels being dependent on pore size.

5. Conclusion

The results from this study provide detailed qualitative and quantitative information on the viscoelastic behavior of PEG-based hydrogels, and thereby provide a broad reference and foundation for a variety of future studies. A hydrogel with desired mechanical properties could potentially be fabricated by selecting appropriate molecular weight and concentration of PEG. Hydrogels with a gradient in composition and mechanical stiffness, mimicking the depth-varying stiffness of cartilage, could also be created. Such hydrogels can be useful to study the functional repair and disruption of damaged articular cartilage and other soft connective tissues.

Acknowledgments

This work was supported by grants from the National Institute of Health.

References

1. Bryant SJ, Anseth KS, Lee DA, Bader DL. Crosslinking density influences the morphology of chondrocytes photoencapsulated in PEG hydrogels during the application of compressive strain. J Orthop Res. 2004; 22:1143–9. [PubMed: 15304291]
2. Nicodemus GD, Bryant SJ. Mechanical loading regimes affect the anabolic and catabolic activities by chondrocytes encapsulated in PEG hydrogels. Osteoarthritis Cartilage. 2010; 18:126–37. [PubMed: 19748607]
3. Troken A, Marion N, Hollister S, Mao J. Tissue engineering of the synovial joint: the role of cell density. Proc Inst Mech Eng H. 2007; 221:429–40. [PubMed: 17822145]
4. Williams CG, Kim TK, Taboas A, Malik A, Manson P, Elisseeff J. In vitro chondrogenesis of bone marrow-derived mesenchymal stem cells in a photopolymerizing hydrogel. Tissue Eng. 2003; 9:679–88. [PubMed: 13678446]
5. Nguyen LH, Kudva AK, Saxena NS, Roy K. Engineering articular cartilage with spatially-varying matrix composition and mechanical properties from a single stem cell population using a multi-layered hydrogel. Biomaterials. 2011; 32:6946–52. [PubMed: 21723599]

6. Hwang NS, Varghese S, Li H, Elisseeff J. Regulation of osteogenic and chondrogenic differentiation of mesenchymal stem cells in PEG-ECM hydrogels. Cell Tissue Res. 2011; 344:499–509. [PubMed: 21503601]
7. Elisseeff J, McIntosh W, Anseth K, Riley S, Ragan P, Langer R. Photoencapsulation of chondrocytes in poly(ethylene oxide)-based semi-interpenetrating networks. J Biomed Mater Res. 2000; 51:164–71. [PubMed: 10825215]
8. Bryant SJ, Anseth KS. Controlling the spatial distribution of ECM components in degradable PEG hydrogels for tissue engineering cartilage. J Biomed Mater Res. 2003; 64A:70–9.
9. Pathak C, Sawhney A, Hubbell JA. In situ photopolymerization and gelation of water soluble monomers: a new approach for local administration of peptide drugs. Polym Preprint. 1992; 33:95–6.
10. Flory PJ, Rehner J. Statistical mechanics of crosslinked polymer networks. II. Swelling. J Chem Phys. 1943; 11:521–6.
11. Peppas NA, Bures P, Leobandung W, Ichikawa H. Hydrogels in pharmaceutical formulations. Eur J Pharm Biopharm. 2000; 50:27–46. [PubMed: 10840191]
12. Williamson AK, Chen AC, Masuda K, Thonar EJ-MA, Sah RL. Tensile mechanical properties of bovine articular cartilage: variations with growth and relationships to collagen network components. J Orthop Res. 2003; 21:872–80. [PubMed: 12919876]
13. Chen AC, Bae WC, Schinagl RM, Sah RL. Depth- and strain-dependent mechanical and electromechanical properties of full-thickness bovine articular cartilage in confined compression. J Biomech. 2001; 34:1–12. [PubMed: 11425068]
14. Johannessen W, Elliott DM. Effects of degeneration on the biphasic material properties of human nucleus pulposus in confined compression. Spine. 2005; 30:E724–9. [PubMed: 16371889]
15. Williamson AK, Chen AC, Sah RL. Compressive properties and function-composition relationships of developing bovine articular cartilage. J Orthop Res. 2001; 19:1113–21. [PubMed: 11781013]
16. Mow VC, Kuei SC, Lai WM, Armstrong CG. Biphasic creep and stress relaxation of articular cartilage in compression? Theory and experiments. J Biomech Eng. 1980; 102:73–84. [PubMed: 7382457]
17. Schinagl RM, Gurskis D, Chen AC, Sah RL. Depth-dependent confined compression modulus of full-thickness bovine articular cartilage. J Orthop Res. 1997; 15:499–506. [PubMed: 9379258]
18. Lai WM, Mow VC, Roth V. Effects of nonlinear strain-dependent permeability and rate of compression on the stress behavior of articular cartilage. J Biomech Eng. 1981; 103:61–6. [PubMed: 7278183]
19. Ateshian GA, Warden WH, Kim JJ, Grelsamer RP, Mow VC. Finite deformation biphasic material properties of bovine articular cartilage from confined compression experiments. J Biomech. 1997; 30:1157–64. [PubMed: 9456384]
20. Frank EH, Grodzinsky AJ. Cartilage electromechanics – II. A continuum model of cartilage electrokinetics and correlation with experiments. J Biomech. 1987; 20:629–39. [PubMed: 3611138]
21. Temple MM, Bae WC, Chen MQ, Lotz M, Amiel D, Coutts RD, et al. Age- and site-associated biomechanical weakening of human articular cartilage of the femoral condyle. Osteoarthritis Cartilage. 2007; 15:1042–52. [PubMed: 17468016]
22. Maroudas A, Bullough P. Permeability of articular cartilage. Nature. 1968; 219:1260–1. [PubMed: 5677422]
23. Temenoff JS, Athanasiou KA, LeBaron RG, Mikos AG. Effect of poly(ethylene glycol) molecular weight on tensile and swelling properties of oligo(poly(-ethylene glycol) fumarate) hydrogels for cartilage tissue engineering. J Biomed Mater Res. 2002; 59:429–37. [PubMed: 11774300]
24. Bryant SJ, Chowdhury TT, Lee DA, Bader DL, Anseth KS. Crosslinking density influences chondrocyte metabolism in dynamically loaded photocrosslinked poly(ethylene glycol) hydrogels. Ann Biomed Eng. 2004; 32:407–17. [PubMed: 15095815]
25. Hou Y, Schoener CA, Regan KR, Munoz-Pinto D, Hahn MS, Grunlan MA. Photo-cross-linked PDMSstar-PEG hydrogels: synthesis, characterization, and potential application for tissue engineering scaffolds. Biomacromolecules. 2010; 11:648–56. [PubMed: 20146518]

26. Bryant SJ, Anseth KS. Hydrogel properties influences ECM production by chondrocytes photoencapsulated in poly(ethylene glycol) hydrogels. J Biomed Mater Res. 2002; 59:63–72. [PubMed: 11745538]
27. Lanasa SM, Hoffecker IT, Bryant SJ. Presence of pores and hydrogel composition influences tensile properties of scaffolds fabricated from well-defined sphere templates. J Biomed Mater Res B Appl Biomater. 2011; 96:294–302. [PubMed: 21210509]
28. Bryant SJ, Bender RJ, Durand KL, Anseth KS. Encapsulating chondrocytes in degrading PEG hydrogels with high modulus: engineering gel structural changes to facilitate cartilaginous tissue production. Biotechnol Bioeng. 2004; 86:747–55. [PubMed: 15162450]
29. Lin-Gibson S, Bencherif S, Cooper JA, Wetzel SJ, Antonucci JM, Vogel BM, et al. Synthesis and characterization of PEG dimethacrylates and their hydrogels. Biomacromolecules. 2004; 5:1280–7. [PubMed: 15244441]
30. DeKosky BJ, Dormer NH, Ingavle GC, Roatch CH, Lomakin J, Detamore MS, et al. Hierarchically designed agarose and poly(ethylene glycol) interpenetrating network hydrogels for cartilage tissue engineering. Tissue Eng Part C Methods. 2010; 16:1533–42. [PubMed: 20626274]
31. Metters AT, Anseth KS, Bowman CN. Fundamental studies of a novel, biodegradable PEG-b-PLA hydrogel. Polymer. 2000; 41(3993):4004.
32. Roberts JJ, Earnshaw A, Ferguson VL, Bryant SJ. Comparative study of the viscoelastic mechanical behavior of agarose and poly(ethylene glycol) hydrogels. J Biomed Mater Res B Appl Biomater. 2011; 99:158–69. [PubMed: 21714081]
33. Cloyd JM, Malhotra NR, Weng L, Chen W, Mauck RL, Elliott DM. Material properties in unconfined compression of human nucleus pulposus, injectable hyaluronic acid-based hydrogels and tissue engineering scaffolds. Eur Spine J. 2007; 16:1892–8. [PubMed: 17661094]
34. Tse JR, Engler AJ. Preparation of hydrogel substrates with tunable mechanical properties. Curr Protoc Cell Biol. 2010; chapter 10(Unit 10):6.
35. Zhang C, Aung A, Liao LQ, Varghese S. A novel single precursor-based biodegradable hydrogel with enhanced mechanical properties. Soft Matter. 2009; 5:3831–4.
36. Lin S, Sangaj N, Razafiarison T, Zhang C, Varghese S. Influence of physical properties of biomaterials on cellular behavior. Pharm Res. 2011; 28:1422–30. [PubMed: 21331474]
37. Buxton AN, Zhu J, Marchant R, West JL, Yoo JU, Johnstone B. Design and characterization of poly(ethylene glycol) photopolymerizable semi-interpenetrating networks for chondrogenesis of human mesenchymal stem cells. Tissue Eng. 2007; 13:2549–60. [PubMed: 17655489]
38. Canal T, Peppas NA. Correlation between mesh size and equilibrium degree of swelling of polymeric networks. J Biomed Mater Res. 1989; 23:1183–93. [PubMed: 2808463]
39. Zar, JH. Biostatistical analysis. 2. Englewood Cliffs, NJ: Prentice-Hall; 1984.
40. Kloxin AM, Kloxin CJ, Bowman CN, Anseth KS. Mechanical properties of cellularly responsive hydrogels and their experimental determination. Adv Mater. 2010; 22:3484–94. [PubMed: 20473984]
41. Proctor CS, Schmidt MB, Whipple RR, Kelly MA, Mow VC. Material properties of the normal medial bovine meniscus. J Orthop Res. 1989; 7:771–82. [PubMed: 2677284]
42. Best BA, Guilak F, Setton LA, Zhu W, Saed-Nejad F, Ratcliffe A, et al. Compressive mechanical properties of the human anulus fibrosus and their relationship to biochemical composition. Spine. 1994; 19:212–21. [PubMed: 8153833]
43. Iatridis JC, Setton LA, Foster RJ, Rawlins BA, Weidenbaum M, Mow VC. Degeneration affects the anisotropic and nonlinear behaviors of human anulus fibrosus in compression. J Biomech. 1998; 31:535–44. [PubMed: 9755038]
44. Quinn TM, Dierckx P, Grodzinsky AJ. Glycosaminoglycan network geometry may contribute to anisotropic hydraulic permeability in cartilage under compression. J Biomech. 2001; 34:1483–90. [PubMed: 11672723]
45. Happel J. Viscous flow relative to arrays of cylinders. AIChE J. 1959; 5:174–7.
46. Gloria A, De Santis R, Ambrosio L, Causa F, Tanner KE. A multi-component fiber-reinforced PHEMA-based hydrogel/HAPEX device for customized intervertebral disc prosthesis. J Biomater Appl. 2011; 25:795–810. [PubMed: 20511384]

47. Johnson EM, Berk DA, Jain RK, Deen WM. Hindered diffusion in agarose gels: test of effective medium model. Biophys J. 1996; 70:1017–23. [PubMed: 8789119]

48. Trabbic-Carlson K, Setton LA, Chilkoti A. Swelling and mechanical behaviors of chemically cross-linked hydrogels of elastin-like polypeptides. Biomacromolecules. 2003; 4:572–80. [PubMed: 12741772]

49. Buschmann MD, Gluzband YA, Grodzinsky AJ, Kimura JH, Hunziker EB. Chondrocytes in agarose culture synthesize a mechanically functional extracellular matrix. J Orthop Res. 1992; 10:745–58. [PubMed: 1403287]

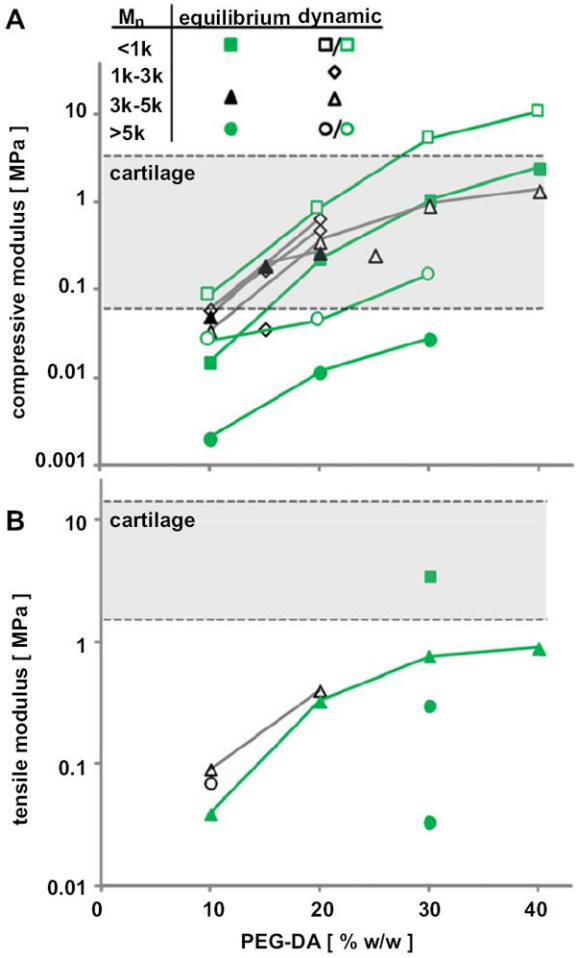

Fig. 1.

Compressive (A) and tensile (B) modulus of PEG hydrogels fabricated from PEG of various concentrations and molecular weights. The modulus was measured at equilibrium (filled symbols) or quasi-static (open symbols) conditions. Data are summarized from previous studies (black) and the current study (green). (For interpretation of color in this figure legend the reader is referred to web version of the article.)

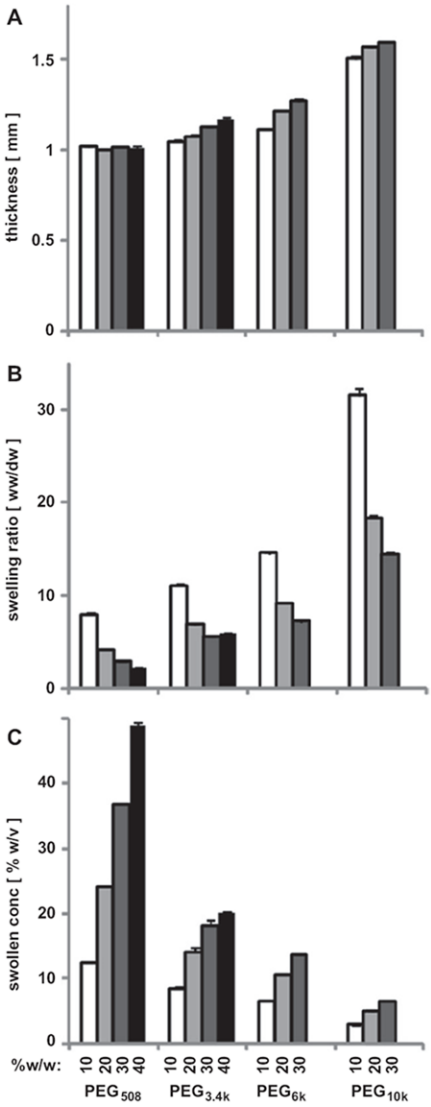

Fig. 2.

Thickness (A), swelling ratio (B), and swollen concentration (C) of PEG hydrogels of different molecular weight (508, 3.4k, 6k, and 10k) and concentrations (10, 20, 30, and 40% w/w) with 0.1% w/w I2959. Data are mean ± SEM (n = 4).

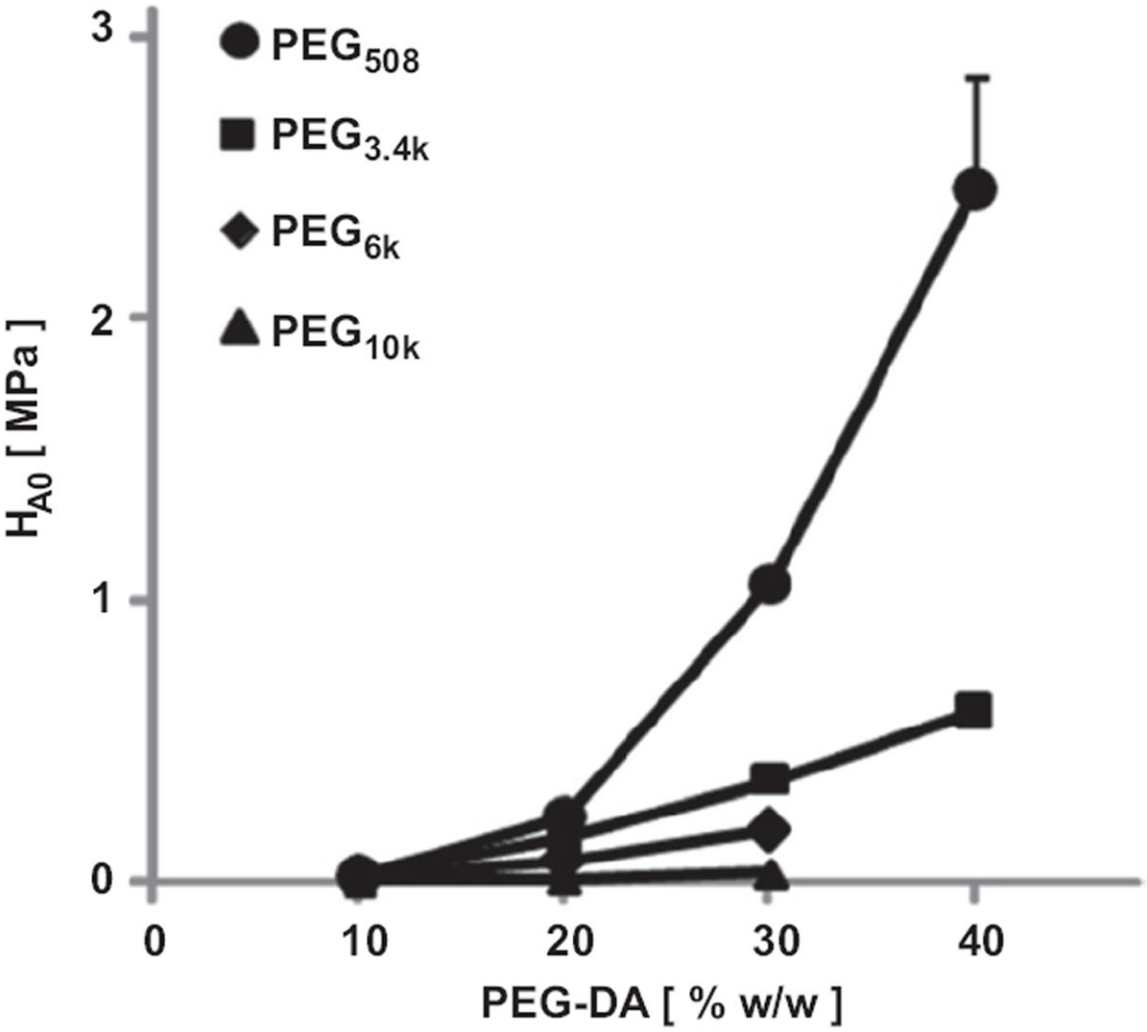

Fig. 3.

Equilibrium CC modulus (H_{A0}) at free swelling thickness of PEG hydrogels of different molecular weight (508 Da, 3.4 kDa, 6 kDa, and 10 kDa) and concentrations (10, 20, 30, and 40% w/w) with 0.1% w/w I2959. Data are mean ± SEM ($n = 4$).

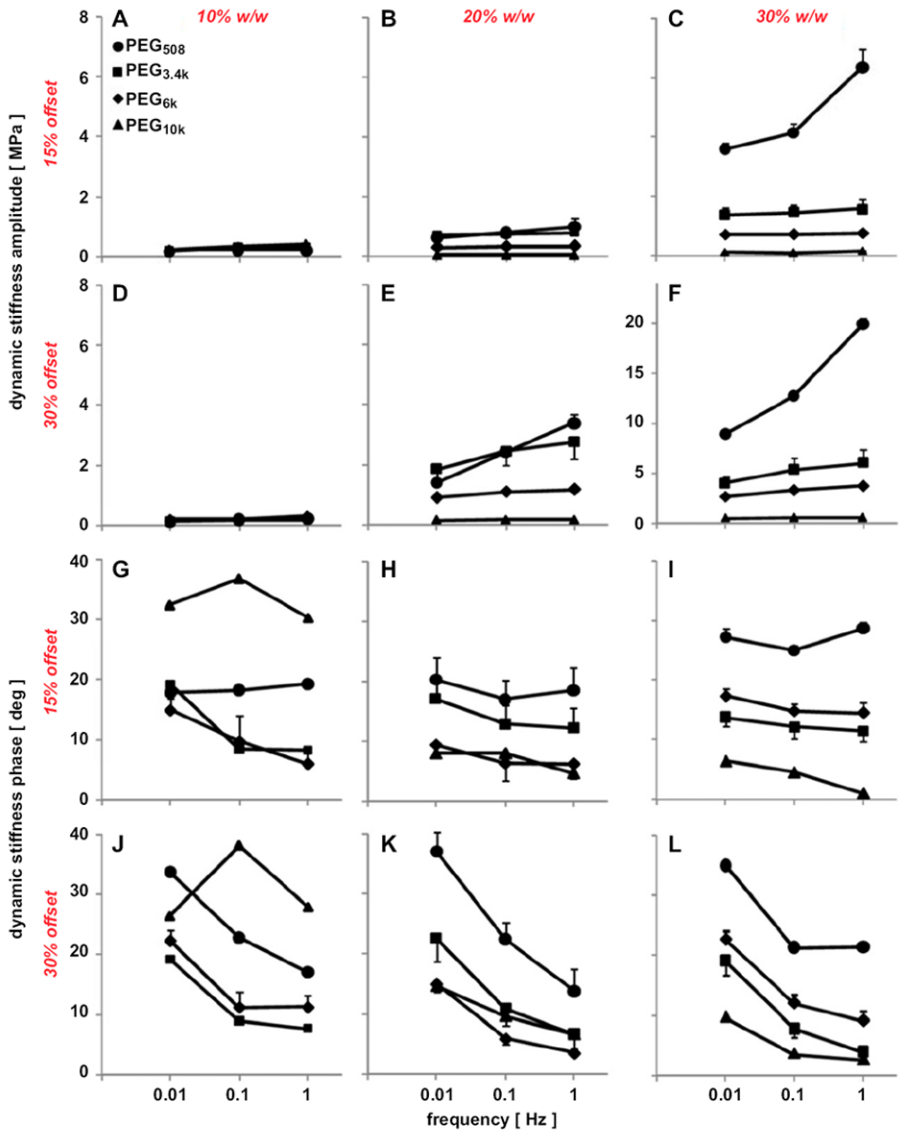

Fig. 4.

Amplitude (A–F) and phase (G–L) of dynamic stiffness of PEG_{508}, $PEG_{3.4k}$, PEG_{6k}, and PEG_{10k} at 10% (A, D, G, J), 20% (B, E, H, K), and 30% w/w (C, F, I, L) with 0.1% w/w I2959. Gels were compressed dynamically with 0.5% amplitude and 0.01, 0.1, and 1 Hz at 15% (A–C, G–I) and 30% (D–F, J–L) static offsets. Data are mean ± SEM ($n = 4$).

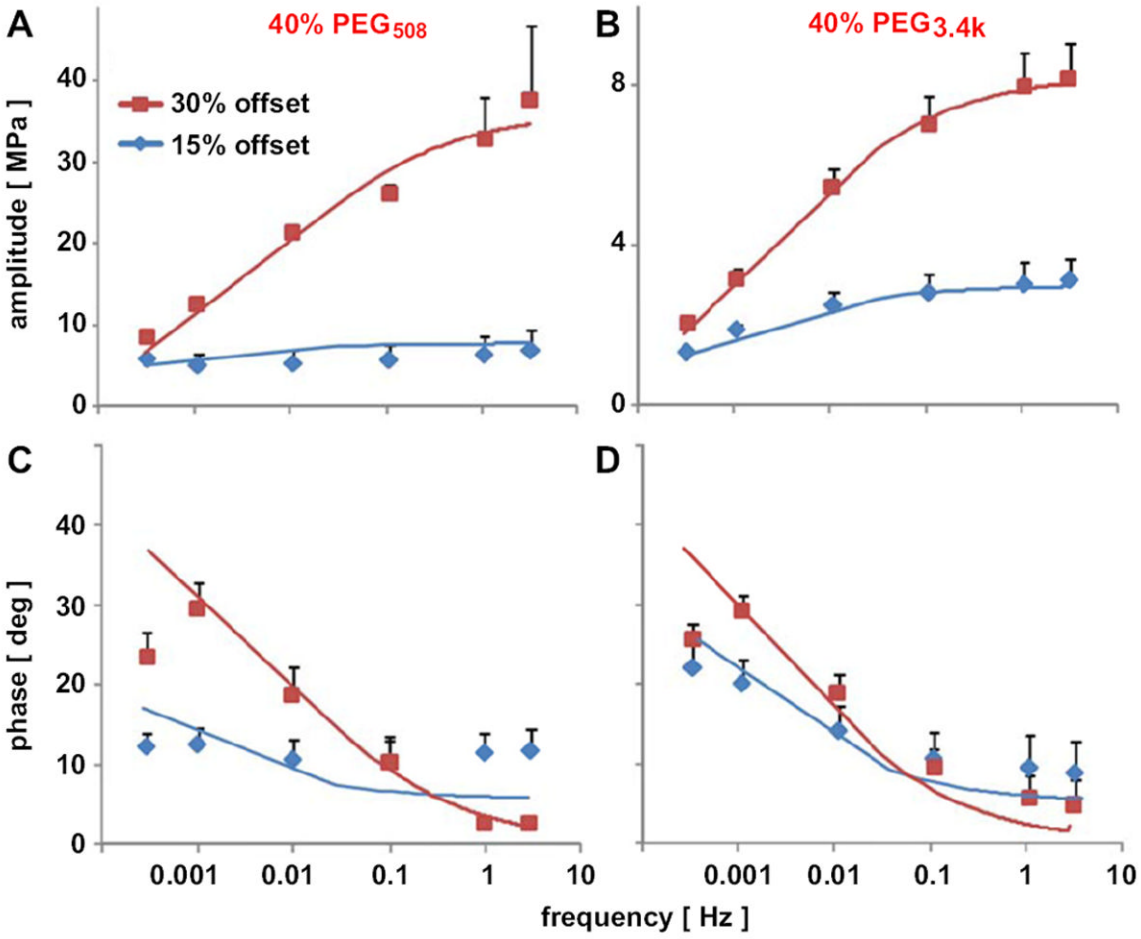

Fig. 5.

Frequency-dependent amplitude (A, B) and phase (C, D) of dynamic stiffness of 40% PEG_{508} (A, C) and $PEG_{3.4k}$ (B, D) hydrogels at 15 and 30% static strain offsets. Gels were compressed dynamically with 0.5% amplitude and 0.0003, 0.001, 0.01, 0.1, 1, and 3 Hz at each static offset. Data are mean ± SEM ($n = 3$).

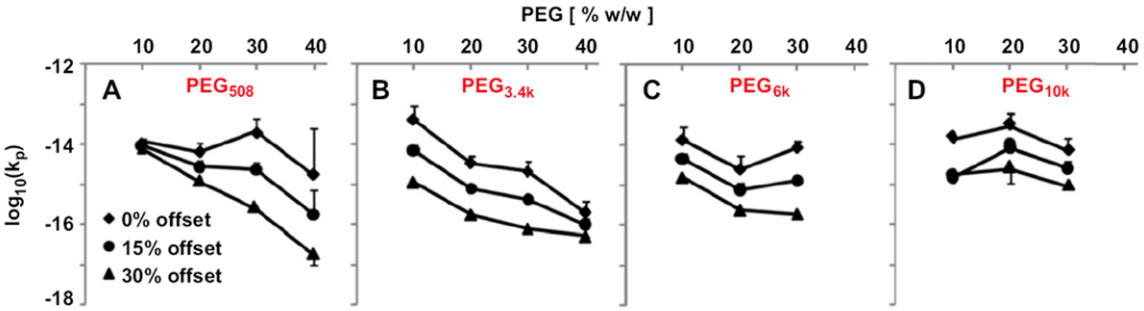

Fig. 6.

Strain-dependent permeability of PEG_{508} (A), $PEG_{3.}$4k (B), PEG_{6k} (C), and PEG_{10k} (D) hydrogels with PEG concentration ranging from 10 to 40% w/w. Samples were compressed dynamically with 0.5% amplitude and 0.01, 0.1, 1 Hz at 15% and 30% compression offsets. Data are mean ± SEM (n = 4).

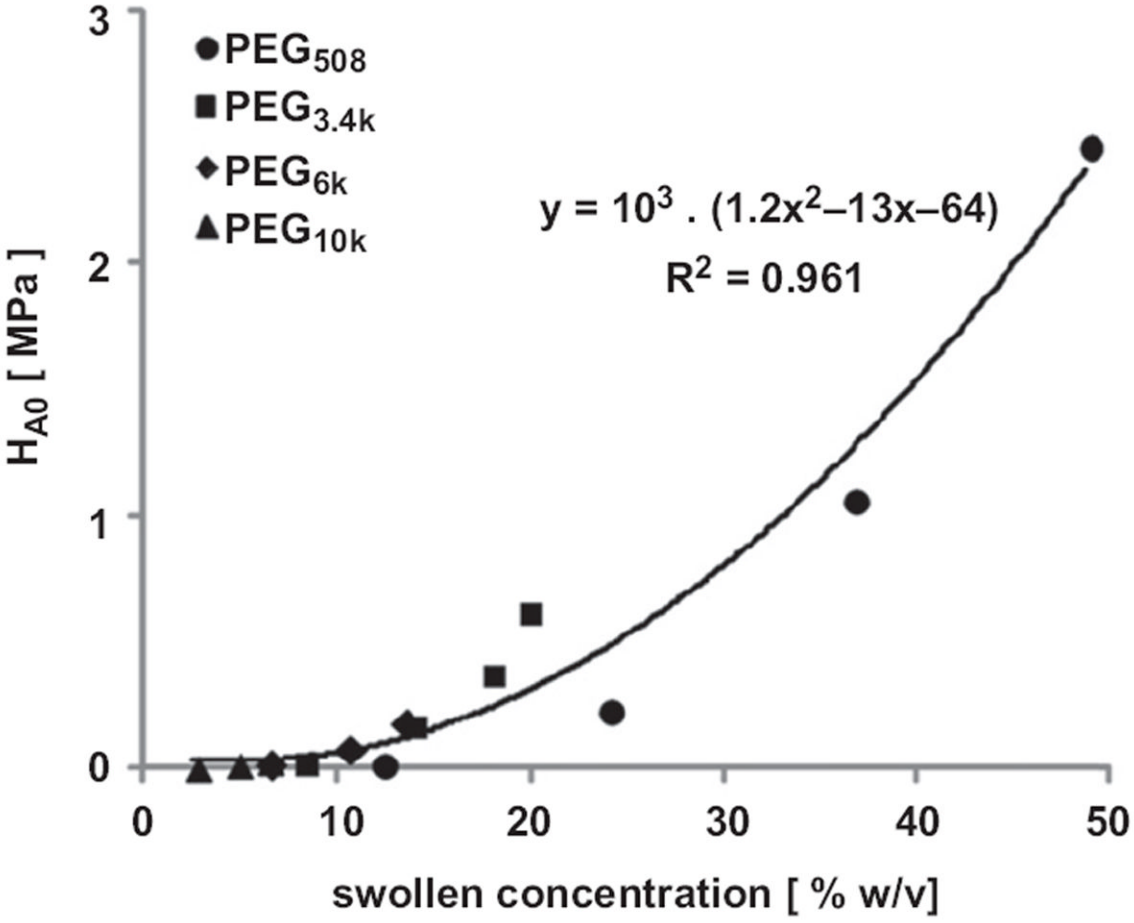

Fig. 7.

Correlation of equilibrium aggregate modulus, H_{A0}, with swollen concentration [%w/v] of PEG diacrylate. Data represent the average of four samples at each molecular weight and concentration ($n = 14$).

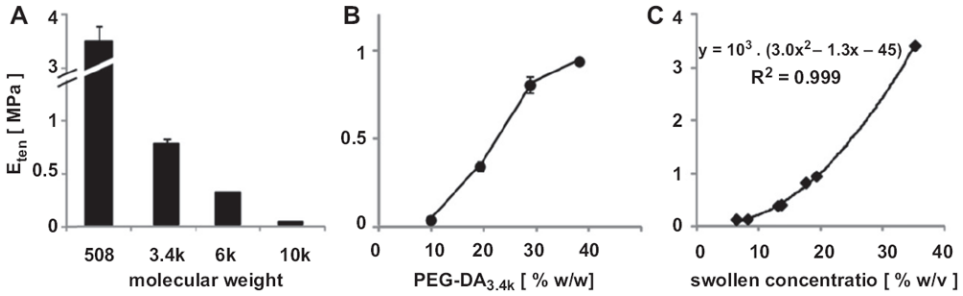

Fig. 8.

Variation of equilibrium tensile modulus, E_{ten}, with PEG molecular weight at 30% (A) and concentration of $PEG_{3.4k}$ (B). E_{ten} of these samples was correlated well with their swollen concentration (C). Data represent mean ± SEM ($n = 4$).

Table 1

Mechanical properties of PEG-based hydrogels in compression and tension [8,23-25,27-32].

PEG formulation	Concentration [%]	Molecular weight [Da]	Methods	Mechanical property determined	Results
[1] PEG-DM	10	3000	15% unconfined compression at constant rate of 0.2; oscillatory compression of 15%, 1 Hz	Tangent modulus, maximum stress from dynamic compression	0.06 MPa, 0.0084 MPa
	20	3000			0.67 MPa, 0.12 MPa
[23] O-PEG-F (OPF)	75	1000	Constant extension at 10 (lk and 4k) or 25 mm/min (10k) until failure	Tensile modulus, stress and strain at fracture	0.09 MPa, 0.025 MPa, 0.31
	75	4000			0.023 MPa, 0.013 MPa, 0.52
	75	10,000			0.016 MPa, 0.013 MPa, 0.77
[25] PEG-DA and $PDMS_{star}$	10	3400	Constant extension at 1 mm/min	Tensile modulus (E)	0.09 MPa
	10	6000			0.07 MPa
[26] PEG-DM	10	3400	Unconfined compression at constant rate of 40 mN/min	Compressive modulus	0.034 MPa
	20	3400			0.36 MPa
	30	3400			0.94 MPa
	40	3400			1.37 MPa
[27] PEG-DA	20	3000	Constant extension at 0.15/min until failure	Quasi-static modulus, ultimate stress and strain	0.4 MPa, 0.2 MPa, 0.37
	65	508			22 MPa, 2.2 MPa, 0.12
	80	508			27 MPa, 1.9 MPa, 0.1
[28] PEG-DM and PEG-LA	10	3000	Unconfined compression at a constant rate of 40–100 mN/min	Compressive modulus	0.06 MPa
	15	3000			0.17 MPa
	20	3000			0.49 MPa
[30] PEG-DA	15	2000	Unconfined compression at constant rate of 0.0005 mm/s until failure	Shear modulus, Young's modulus, stress and strain at failure	0.01 MPa (G), 0.036 MPa (E),0.36 MPa, 0.71
[31] PEG-b-PLA	25	4600	Unconfined compression at constant rate of 400 mN/min	Compressive modulus	0.25 MPa
	50	4600			0.7 MPa
	70	4600			0.9 MPa
[32] PEG-DM	10	4600	Equilibrium unconfined compression at 5–20%; oscillatory compression of 1%, 0.01–10 Hz at 10% offset	Equilibrium compressive modulus and storage modulus	0.05 MPa, 0.04–0.05 MPa
	15	4600			0.19 MPa, 0.15–0.19 MPa
	20	4600			0.27 MPa, 0.25–0.55 MPa

Abbreviations: PEG-diacrylate (PEG-DA), PEG-dimethacrylate (PEG-DM), oligo-(PEG)-fumarate (O-PEG-F), PEG poly (lactic acid) (PEG-b-PLA), PEG-urethane dimethacrylate (PEG-UDM).

Table 2

The effect of molecular weight (M_n) and concentration ([PEG]) of the precursors on water content (% water), average molecular weight between crosslinks (M_c) and mesh size (ξ) of PEG hydrogels. Hydrogels were fabricated and analyzed for structural properties, using the Peppas–Merrill model as described previously [36-38]. Data are mean ± SEM.

PEG type	PEG M_n	% PEG	% Water	M_c [g/mol]	ξ [nm]
PEG_{508}	508	10	87.5 ± 0.2	167 ± 3	1.70 ± 0.03
PEG_{508}	508	20	75.9 ± 0.1	107 ± 1	1.09 ± 0.01
PEG_{508}	508	30	65.0 ± 0.2	72 ± 1	0.79 ± 0.01
PEG_{508}	508	40	55.1 ± 0.1	50 ± 1	0.61 ± 0.01
$PEG_{3.4k}$	3400	10	91.0 ± 0.2	701 ± 22	3.87 ± 0.09
$PEG_{3.4k}$	3400	20	85.4 ± 0.4	539 ± 27	2.90 ± 0.10
$PEG_{3.4k}$	3400	30	82.1 ± 0.3	503 ± 14	2.61 ± 0.05
$PEG_{3.4k}$	3400	40	83.0 ± 0.2	661 ± 11	3.05 ± 0.04
PEG_{6k}	6000	10	93.1 ± 0.1	1313 ± 10	5.81 ± 0.03
PEG_{6k}	6000	20	89.1 ± 0.1	1056 ± 13	4.47 ± 0.04
PEG_{6k}	6000	30	86.1 ± 0.1	931 ± 6	3.87 ± 0.02
PEG_{10k}	10,000	10	96.8 ± 0.1	3556 ± 49	12.37 ± 0.18
PEG_{10k}	10,000	20	94.5 ± 0.1	2986 ± 45	9.45 ± 0.13
PEG_{10k}	10,000	30	93.1 ± 0.1	2809 ± 26	8.48 ± 0.07